ChemComm

# Copper Metal Electrode Reversibly Hosts Fluoride in a 16 m KF Aqueous Electrolyte



| | |
|---|---|
| Journal: | *ChemComm* |
| Manuscript ID | CC-COM-05-2022-002978.R1 |
| Article Type: | Communication |
| | |

COMMUNICATION

# Copper Metal Electrode Reversibly Hosts Fluoride in a 16 *m* KF Aqueous Electrolyte

Received 00th January 20xx,
Accepted 00th January 20xx

DOI: 10.1039/x0xx00000x

Trenton C. Gallagher,[a] Sean K. Sandstrom,[a] Che-Yu Wu,[a] William Stickle,[b] Calvin R. Fulkerson,[a] Lindsey Hagglund,[a] and Xiulei Ji*[a]

**Fluoride is a promising charge carrier for batteries due to its high charge/mass ratio and small radius. Here, we report commercial copper powder exhibits a reversible capacity of up to 222 mAh/g in a saturated electrolyte of 16 *m* KF. This electrolyte suppresses dissolution of $CuF_2$, the charged product. Furthermore, the KF solid comprised in the Cu electrode facilitates a high initial capacity. Our results showcase the potential of aqueous fluoride batteries using copper as an electrode.**

Recently, fluoride has emerged as a charge carrier for anion rocking-chair batteries. Fluoride possesses an ionic radius of 133 pm, only larger than hydride, as the second smallest among all common anions.[1] Fluorine is also one of the most earth-abundant elements, with an abundance of 611 ppm in contrast to 22 ppm for lithium.[2] These characteristics are attractive for alternative battery technologies utilizing fluoride as a charge carrier. Reddy and Fichtner reported the first fluoride battery chemistry in 2011, which used a solid-state electrolyte, a bismuth fluoride as the cathode, and metallic cerium as the anode.[3] To date, fluoride battery research has been mostly associated with solid-state electrolytes.[4,5,6] However, solid-state electrolytes are limited by low ionic conductivities in the orders of $10^{-5}$–$10^{-4}$ S $cm^{-1}$.[7] The low ionic conductivity at room temperature hinders the performance so that the cells must operate at high temperatures, typically over 150 ˚C, in order to provide meaningful capacity and cycle life.[8] In 2018, Davis *et al.* reported a room-temperature fluorinated-ether electrolyte that facilitates the reversible fluoride insertion in a Cu/$LaF_3$ core-shell electrode.[9] Unfortunately, the electrode delivers a limited capacity of less than 70 mAh/g with limited cycle life. In addition, ionic liquids have been explored as electrolytes for fluoride insertion.[10,11]

Compared with other electrolytes, aqueous electrolytes tend to possess attributes of high ionic conductivity, low cost, and environmental friendliness. Most recently, aqueous fluoride electrolytes have raised attention, where dilute NaF and KF electrolytes have been explored for the electrodes of $BiF_3$.[12,13,14] KF has a high solubility of 16 *m* in an aqueous solution at room temperature. This high concentration classifies this electrolyte as a "water in salt" electrolyte.[15] Nevertheless, it has yet to be demonstrated as an effective electrolyte for fluoride-hosting electrodes.

To date, few fluoride-hosting electrode materials have been reported, and usually the initial compositions of the electrodes are metal fluorides such as $CuF_2$,[3] $BiF_3$[6], and $PbF_2$[16]. In fact, metals can be used as the starting electrodes as well. Nakano *et al.* reported that Cu cathode exhibits a near theoretical capacity of 820 mAh/g at 150 ˚C with a $LaF_3$ solid-state electrolyte.[4] Copper is thermodynamically stable in aqueous fluoride electrolytes; however, its fluoride incorporation properties have yet not been demonstrated. Another challenge is that $CuF_2$ the charged product is soluble in aqueous electrolytes with a maximum concentration of 0.46 M at room temperature. The as-formed $CuF_2$ during charge can be dissolved in the electrolyte, causing a shuttling effect due to self-discharge with the counter electrode.

Herein, we report reversible fluoride storage properties of commercial copper powder (625 mesh) in a "water in salt" electrolyte of 16 *m* KF ($KF{\cdot}3.47H_2O$). This new electrolyte allows the reversible conversion reaction between Cu and $CuF_2$ by mitigating the dissolution problem for the active mass. Furthermore, the KF saturated electrolyte allows the addition of KF solid in the Cu electrode as a part of the active mass, which helps the Cu electrode deliver a high capacity of over 200 mAh/g and a long cycle life.

We employed three-electrode cells to investigate the electrochemical properties of the Cu working electrode with a Cu active mass loading of 20 mg/$cm^2$, where Ag/AgCl and a freestanding film of activated carbon with a mass loading of 200 mg/$cm^2$ are employed as reference and counter electrodes. We

[a] *Department of Chemistry, Oregon State University Corvallis, Oregon 97331-4003, United States. Email: david.ji@oregonstate.edu*
[b] *Hewlett-Packard Co., 1000 NE Circle Blvd., Corvallis, Oregon, 97330, United States*
† Footnotes relating to the title and/or authors should appear here.
Electronic Supplementary Information (ESI) available: [details of any supplementary information available should be included here]. See DOI: 10.1039/x0xx00000x

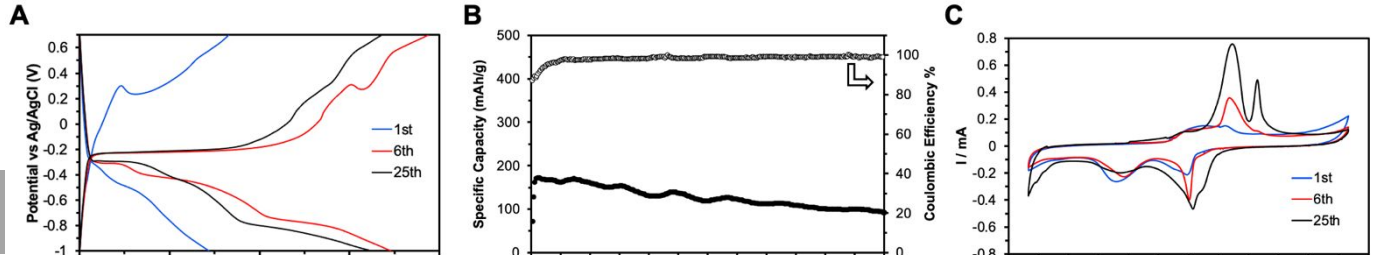

first evaluated the copper electrode in a dilute 1 *m* KF electrolyte. As shown in **Figure S1**, the galvanostatic charge-discharge (GCD) profiles show a typical shuttling mechanism during the first charge with a prolonged charging profile, which can be attributed to the dissolution of the as-formed $CuF_2$. In contrast, in 16 *m* KF, the Cu electrode shows a reversible oxidation/reduction behavior (**Figure 1A**). In this electrode, the Cu electrode provides the first discharge capacity of 72 mAh/g with largely sloping GCD profiles and an initial Coulombic efficiency (CE) of 87%. The initial cycling demonstrates a conditioning process, where the capacity continuously increases and reaches its maximum of 173 mAh/g in the sixth cycle. After conditioning, the electrode maintained an average CE of 98.4% and exhibited a capacity retention of 54% after 300 cycles (**Figure 1B**), one of the most stable cycling performances for fluoride batteries. The conditioning may involve roughening up the structure of the copper particles so that active mass is more accessible to fluoride ions.[17] Interestingly, the charging profiles transition from a slope in the first cycle to a combination of a flat plateau and a slope. In addition, the discharge behaviors also change from a slope to staired profiles with plateaus, where the overall extent of polarization decreases over cycling.

As shown in **Figure 1C**, the first anodic scan in cyclic voltammetry (CV) shows a broad and weak peak from -0.4 V to -0.1 V (vs. Ag/AgCl, hereafter). The cathodic scan shows two peaks at -0.3 V and -0.65 V. Over more scans, the peak intensity of both anodic and cathodic peaks increases, corroborating the existence of a conditioning process. The anodic peaks shift to a higher potential at the 6$^{th}$ and 25$^{th}$ cycle, and a shoulder peak at the higher potential turns more resolved progressively. For the cathodic peaks, the intensity of the peak at ca. -0.6 V decreases, and the peak at -0.3 V gets strengthened over cycling. Overall, the weight of cathodic peaks shifts to a higher potential, reducing the polarization, which is aligned with the GCD results.

The multiple peaks in CV and staired plateaus in the GCD profiles may have to do with a surface layer of copper oxides. It was reported that in a neutral pH environment spontaneous passivation of copper occurs, forming a surface layer of $Cu_2O$.[18,19] Considering the pH value of the 16 *m* KF is ca. 8.3, the same surface passivation layer can be formed. Note that such a passivating layer may hinder fluoride's ability to navigate to the incorporation sites of the copper electrode, preventing the electrode from achieving a high capacity during the initial conditioning process. The question is whether $Cu_2O$ can be oxidized to $CuF_2$ at the end of charging. We characterized the charged electrode. *Ex situ* X-ray diffraction (XRD) pattern shows that the charging process generates a pure phase of monoclinic $CuF_2$ (PDF #06-143), where $Cu_2O$ or CuO phase cannot be identified.[20] (**Figure 1D**). It should be noted that peaks at 44˚ and 75˚ correspond to the unreacted copper. Upon discharge, the electrode converts back to copper (**Figure S3)**. To further characterize the charged product, X-ray photoelectron spectroscopy (XPS) was employed to identify the species residing on the surface of the electrode. Results indicate that $CuF_2$ is the primary product on the surface after charging (**Figure 1E).** The peak doublet of the Cu $2p_{3/2}$ and Cu $2p_{1/2}$ components at 933 and 954 eV can be assigned to Cu (II) coordinated to fluoride. The other doublet, with peaks centered at 943 and 963 eV, correlate to the shake-up satellites, characteristic for Cu(II) as well.[21] The mechanism is illustrated in equation 1.

$$Cu\ (s) + 2F^-\ (aq) \leftrightarrow CuF_2\ (s) + 2e^- \quad (1)$$

After cycling, the cell was disassembled, and a blue residue was observed on the separator (**Figure S2**), which is confirmed as monoclinic $CuF_2$ by XRD (**Figure S4**). The presence of $CuF_2$ on the separator suggests the fading mechanism: during charging, the formation of the copper fluoride consumes electrolyte ions, which renders the electrolyte unsaturated; therefore, it is possible that the as-formed $CuF_2$ may dissolve into the electrolyte. Another factor is the volume expansion from Cu to $CuF_2$ by 238% that may result in the poor structural integrity of the electrode, where the binder cannot effectively secure the swollen active mass.

The Cu electrode operates by incorporating incoming fluoride from the electrolyte. A challenge is the lowered electrolyte concentration in this configuration of dual-ion battery (DIB). Here, the saturated KF electrolyte allows us to convert the Cu electrode from a DIB cathode to an electrode of rocking-chair batteries by adding KF salt solid into the copper electrode. With KF on board, the incorporation of fluoride by Cu during charge can be facilitated locally by KF dissolution, where it is the K-ions that commute to the counter electrode to meet the charge neutrality of both electrodes. During discharge, KF will precipitate on the surface of the electrode. The KF solid will maintain the overall concentration of the electrolyte constant, where potentially the battery can use a minimal volume of the electrolyte.

We added the amount of KF solid to the copper electrode to provide ions needed for a charging capacity of 300 mAh/g based on the mass of copper electrode. By introducing KF in the

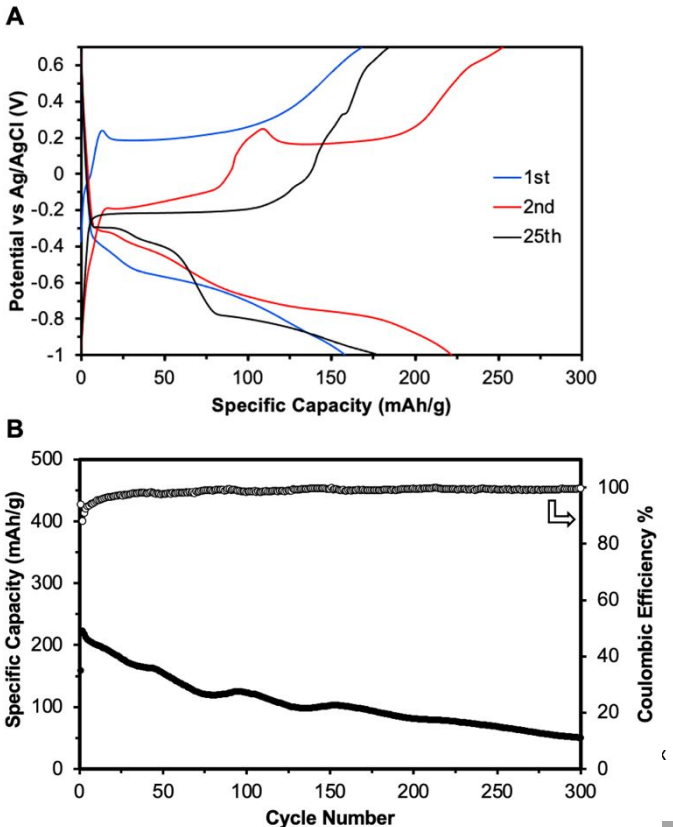


**Figure 2. Electrochemical performance of CuK in 16 m KF.** (**A**) GCD potential profiles of the 1$^{st}$,10$^{th}$, and 25$^{th}$ cycle at 500 mAh/g. (**B**) Cycling performance.

electrode, the first discharge capacity of the electrode is increased to 158 mAh/g (based on the mass of copper), much larger than the case without KF salt added (**Figure 2A**). In addition, the previously observed conditioning is largely shortened, where in the second discharge, the capacity goes up to 222 mAh/g. Unfortunately, the overall capacity retention for the electrode with KF on board is not more competitive. After 300 cycles, the electrode retains a discharge capacity of 50 mAh/g (**Figure 2B**). The capacity fading may be related to the uncontrolled precipitation of KF on the electrode surface and the unregulated volumetric changes.

In summary, a highly concentrated KF electrolyte was first employed to enable copper metal as a fluoride-ion electrode. This effective strategy unlocked the highly reversible cycling of the copper electrode with a capacity retention of (54%) over 300 cycles. With KF embedded into the electrode, the Cu electrode exhibits a maximum capacity of 222 mAh/g in the second cycle. This work shows the potential of an aqueous fluoride ion battery where the transition metals can serve as electrodes.

X. J. is grateful for the financial support from the U.S. National Science Foundation (NSF), Award No. 2038381.

## Conflicts of interest

There are no conflicts of interest to declare.

## Notes and references

§ HF vapor may be generated from the 16 *m* KF electrolyte. Caution should be taken when handling this concentrated solution and the used electrochemical cells containing it.

1 R. D. Shannon, *Acta Crystallographica,* 1976, **32**, 751–767.
2 M. G. García, L. Borgnino, *Royal Society of Chemistry*, 2015, **1**, 3-21.
3 M. Anji Reddy, M. Fichtner, *Journal of Materials Chemistry,* 2011, **21**(43), 17059-17062.
4 D. Tho Thieu, M. H. Fawey, H. Bhatia, T. Diemant, V. S. K. Chakravadhanula, R. J. Behm, C. Kübel, M. Fichtner, *Advanced Functional Materials,* 2017, **27**(31), 1701051.
5 H. Nakano, T. Matsunaga, T. Mori, K. Nakanishi, Y. Morita, K. Ide, K. Okazaki, Y. Orikasa, T. Minato, K. Yamamoto, Z. Ogumi, Y. Uchimoto, *Chemistry of Materials*, 2021, **33**(1), 459-466.
6 I. Mohammed, R. Witter, M. Fichtner, M. Anji Reddy, *ACS Applied Energy Materials*, 2018, **1**(9), 4766-4775.
7 C. Rongeat, M. Anji Reddy, R. Witter, M. Fichtner, *ACS Applied Materials & Interface*, 2014, **6**(3), 2103-2110.
8 S. K. Sandstrom, X. Chen, X. Ji, *Carbon Energy*, 2021, **3**(4), 627-653.
9 V. K. Davis, C. M. Bates, K. Omichi, B. M. Savoie, N. Momčilović, Q. Xu, W. J. Wolf, M. A. Webb, K. J. Billings, N. H. Chou, S. Alayoglu, R. K. McKenney, I. M. Darolles, N. G. Nair, A. Hightower, D. Rosenberg, M. Ahmed, C. J. Brooks, T. F. Miller III, R. H. Grubbs, S. C. Jones, *Science*, 2018, **362**(6419), 1144-1148.
10 I. Darolles, C. M. Weiss, M. M. Alam, A. Tiruvannamalai, S. C. Jones, *California Institute of Technology,* 2015.
11 T. Yamamoto, K. Matsumoto, R. Hagiwara, T. Nohira, *ACS Applied Energy Materials,* 2019, **2**(9), 6153-6157.
12 X. Hou, Z. Zhang, K. Shen, S. Cheng, Q. He, Y. Shi, D. Y. W. Yi, C. Su, L. Li, F. Chen, *The Electrochemical Society,* 2019, **166**(12), A2419.
13 Z. Zhang, X. Hu, Y. Zhou, S. Wang, L. Yao, H. Pan, C. Su, F. Chen, X. Hou, *Journal of Materials Chemistry A*, **6**(18), 8244-8250.
14 X. Li, Y. Tang, J. Zhu, H. Lv, Y. Hu, W. Wang, C. Zhi, H. Li, *Advance Energy Materials*, 2021, **11**(14).
15 L. Suo, O. Borodin, Y. Wang, X. Rong, W. Sun, X. Fan, S. Xu, M. A. Schroeder, A. V. Cresce, F. Wang, C. Yang, Y. Hu, K. Xu, C. Wang, *Advanced Energy Materials*, 2017, **7**(21), 1701189.
16 H. Konishi, T. Minato, T. Abe, Z. Ogumi, *Journal of Electroanalytical Chemistry*, 2018, **826**, 60-64.
17 H. Wang, T. Liang, M. Gong, Y. Li, W. Chang, T. Mefford, J. Zhou, J. Wang, T. Regier, F. Wei, H. Dai, *Nature Communications*, 2012, **3**, 1-8.
18 Y. Feng, K. Siow, W. Teo, K. Tan, A. Hsieh, *Corrosion*, 1997, **53**(5).
19 G. Gao, B. Yuan, C. Wang, L. Li, S. Chen, *International Journal of Electrochemical Science*, 2014, **9**, 2565-2574.
20 C. M. Wheeler, H. M. Haendler, *Journal of the American Chemical Society*, 1954, **76**, 264-264.
21 G. van der Laan, C. Westra, C. Haas, G. A. Sawatzky, *Physical Review B,* 1981, **23**(9), 4369-4380.
22 A. W. Xiao, G. Galatolo, M. Pasta, *Perspective*, 2021, **5**(11), P2823-2844.